Electronic Supplementary Information (ESI) for the New Journal of Chemistry

Electronic Supplementary Information

Enhanced Analytical and Physical Characterization of Mixtures of Random Bay-Position Chlorinated Boron Subnaphthalocyanines Enabled by an Established Partial Separation Method (a Part 2).

Devon P. Holst[a] *and Timothy P. Bender**[a,b,c]

[a] Department of Chemistry, University of Toronto, 80 St. George Street, Toronto, Ontario, Canada M5S 3H6

[b] Department of Chemical Engineering and Applied Chemistry, University of Toronto, 200 College Street, Toronto, Ontario, Canada M5S 3E5

[c] Department of Materials Science and Engineering, University of Toronto, 184 College Street, Toronto, Ontario, Canada M5S 3E4

* to whom correspondences should be addressed. Email: tim.bender@utoronto.ca

Table of Contents **Page #**

List of Figures **Page #**

List of Tables **Page #**

Materials

Dichloromethane, hexanes, toluene, N,N-dimethylformamide (distilled in glass), acetonitrile (HPLC-grade), and sodium iodide were purchased from Caledon Labs (Caledon, Ontario, Canada) and used without further purification unless otherwise stated. Fumaronitrile was purchased from TCI America (Portland, Oregon, USA) and used as received. Boron trichloride (1.0 M in heptane), sodium bisulfite, oxazine 170, decamethylferrocene, red phosphorus, tetrabutylammonium perchlorate, and acetone-d_6 were purchased from Sigma-Aldrich Chemical Company (Mississauga, Ontario, Canada) and used as received. α,α,α',α'-Tetrabromo-o-xylene was purchased from Leap Labchem Company Limited (Hangzhou, China) and used as received. Aluminum plates coated with silica (pore size of 60Å) and fluorescent indicator were purchased from Whatman International Ltd. (Kent, England). Flash Silica Gel P60 (mesh size 40-63 µm) and glass plates coated with reverse phase silica was purchased from SiliCycle Inc. (Quebec City, Quebec, Canada). Pentafluorophenol was purchased from Oakwood Products Inc (Estill, South Carolina, USA) and used as received. 2,5-Dihydroxybenzoic acid was purchased from Bruker (Massachusetts, USA) and used as received.

Instrumentation

Photoluminescence (PL) spectra were measured using a PerkinElmer LS 55 in toluene at room temperature. Fluorescence quantum yields were calculated using equation S3. Ultraviolet-visible (UV-Vis) spectroscopy was conducted with a PerkinElmer LAMBDA 1050 using a PerkinElmer quartz cuvette with a 10 mm path length. High-performance liquid chromatography (HPLC) analysis was conducted using a Waters 2695 separation module with a Waters 2998 photodiode array fitted with a SunFire^{TM} C18 3.5 µm 3.0 x 150 mm column. HPLC grade acetonitrile and distilled in glass N,N-dimethylformamide were used as the mobile phase eluted at 0.6 mL/min at a composition of 80:20 (v:v). Cyclic voltammetry (CV) and differential pulse voltammetry (DVP) was conducted using a Basi EC-Epsilon potentiostat/galvanostat with the C-3 Cell Stand. The working electrode was a 1 mm glassy carbon, the counter electrode was a platinum wire, and the reference electrode was Ag/AgCl saturated salt solution. Spec-grade solvents were purged with nitrogen gas at room temperature prior to their use. Four cycles at a scan rate of 100 mV/s were measured for each sample. Tetrabutylammonium perchlorate (0.1 M) was used as the supporting electrolyte. Decamethylferrocene was used as an internal reference. All half-wave potentials were corrected to the half-wave reduction potential ($E_{1/2,red}$) of decamethylferrocene, which was previously reported to be -0.012 V vs. Ag/AgCl.[1] Nuclear magnetic resonance (NMR) spectra were generated using a 700 MHz Agilent DD2 NMR Spectrometer with a cryogenically cooled probe when a 700 MHz working frequency is referenced. NMR spectra were generated using a 500 MHz Agilent DD2 NMR Spectrometer with a cryogenically cooled probe when a 500 MHz working frequency is referenced. Spectra are referenced to the deuterated solvent peak (acetone-d_6 δ 2.050 ppm). Spin multiplicities are designated by the following abbreviations: s (singlet), d (doublet), t (triplet), q (quartet) and m (multiplet). Laser desorption/ionization mass spectrometry LDI and matrix-assisted laser desorption/ionization mass spectrometry (MALDI MS) was conducted using a Bruker Autoflex Speed matrix-assisted laser desorption ionization time-of-flight mass spectrometer (MALDI-TOF-MS) with a 3rd harmonic Nd:YAG laser @ 355 nm. MALDI and LDI was run in positive ion mode and calibrated using red phosphorus.

Column Chromatography Mass Flow

Table S1. Mass of F_5-Cl_nBsubNc Collected from Column Chromatography

F5-ClnBsubNc Band	Mass	% of loaded mass
0	<1	<0.5
1	4	2
2	18	9
3	27	13.5

200 mg of F_5-Cl_nBsubNc was loaded onto the column. The mass of bands 1, 2, and 3 represent a 24.5% mass recovery.

Nuclear Magnetic Resonance

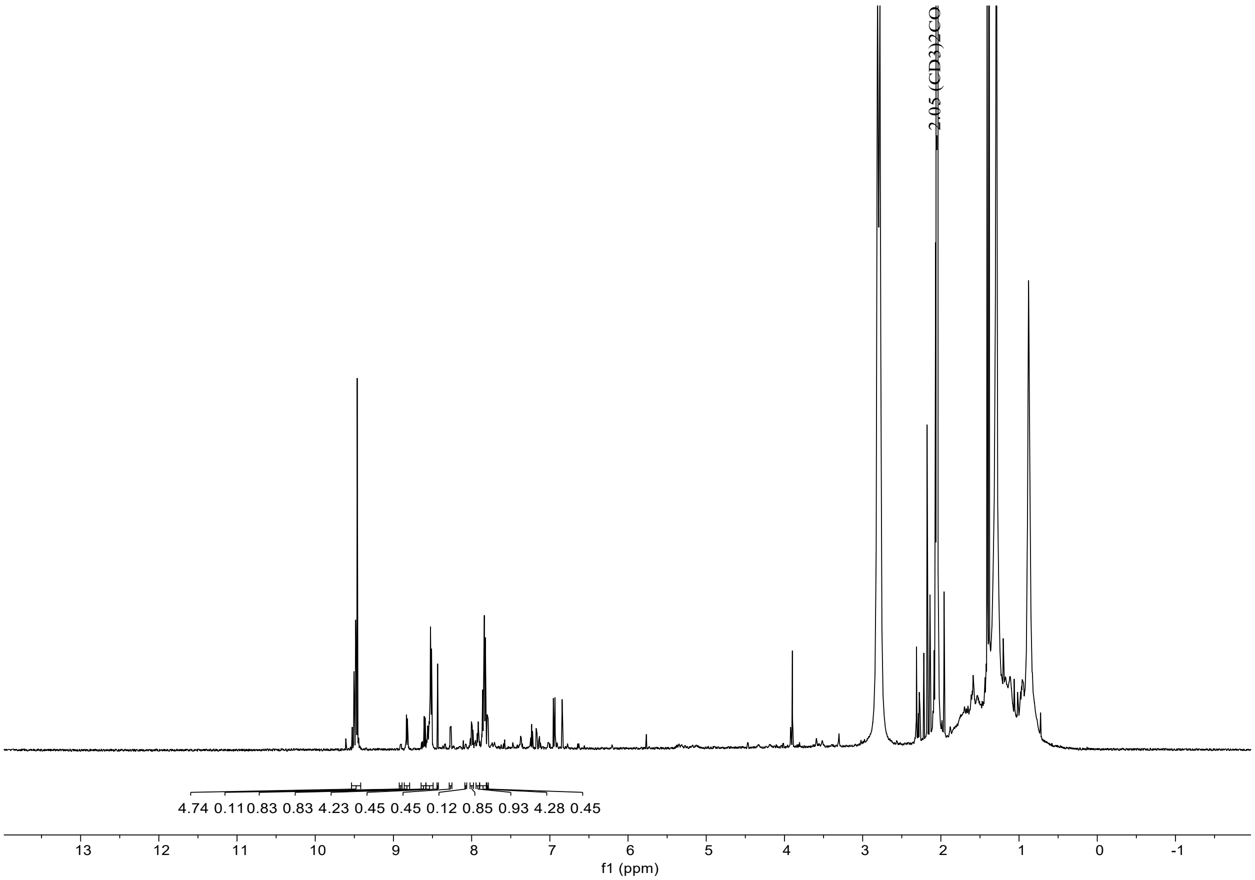

Figure S1. ^{1}H NMR spectrum (700 MHz) of F_5-Cl_nBsubNc crude.

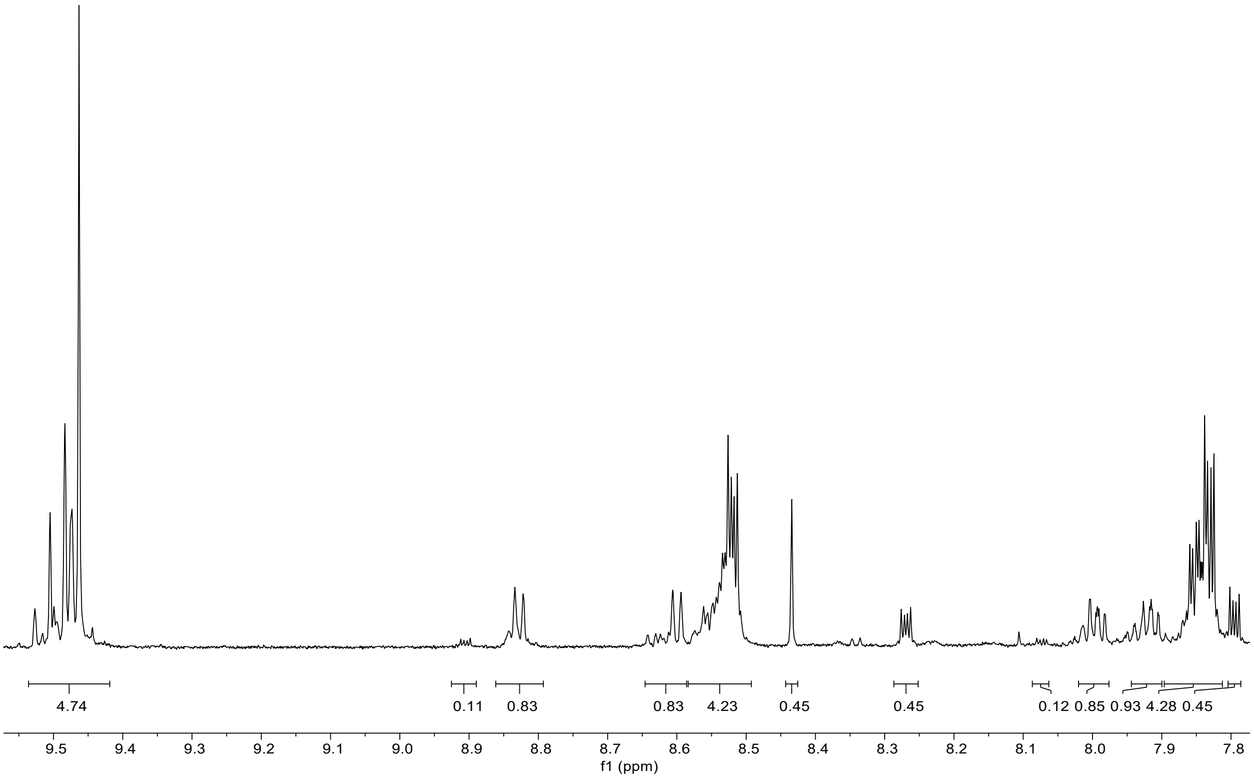

Figure S2. Zoom of the ^{1}H NMR spectrum of F_5-Cl_nBsubNc crude. Peaks with integrations of 0.45 are from the presence of the precursor 2,3-DCN.

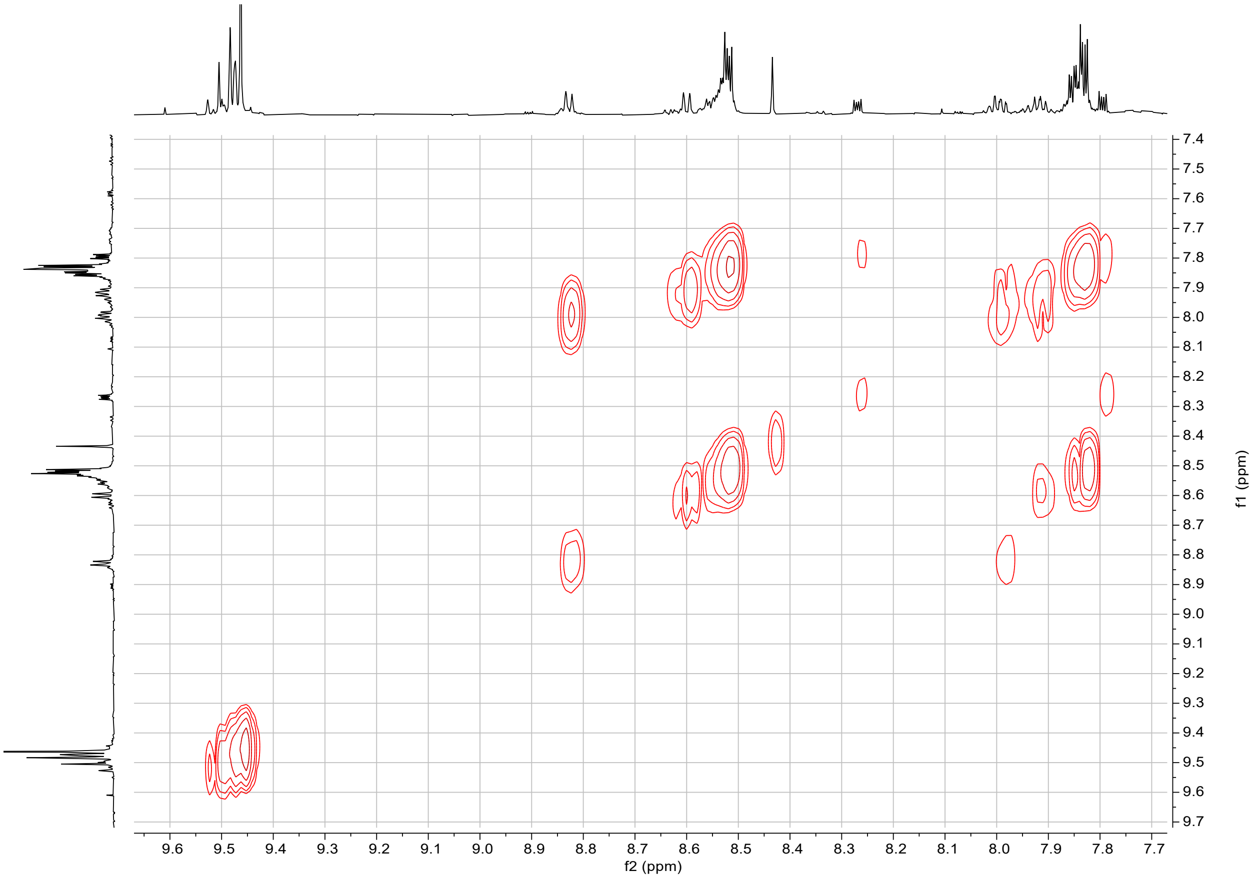

Figure S3. COSY NMR of F$_5$-Cl$_n$BsubNc crude (700 MHz).

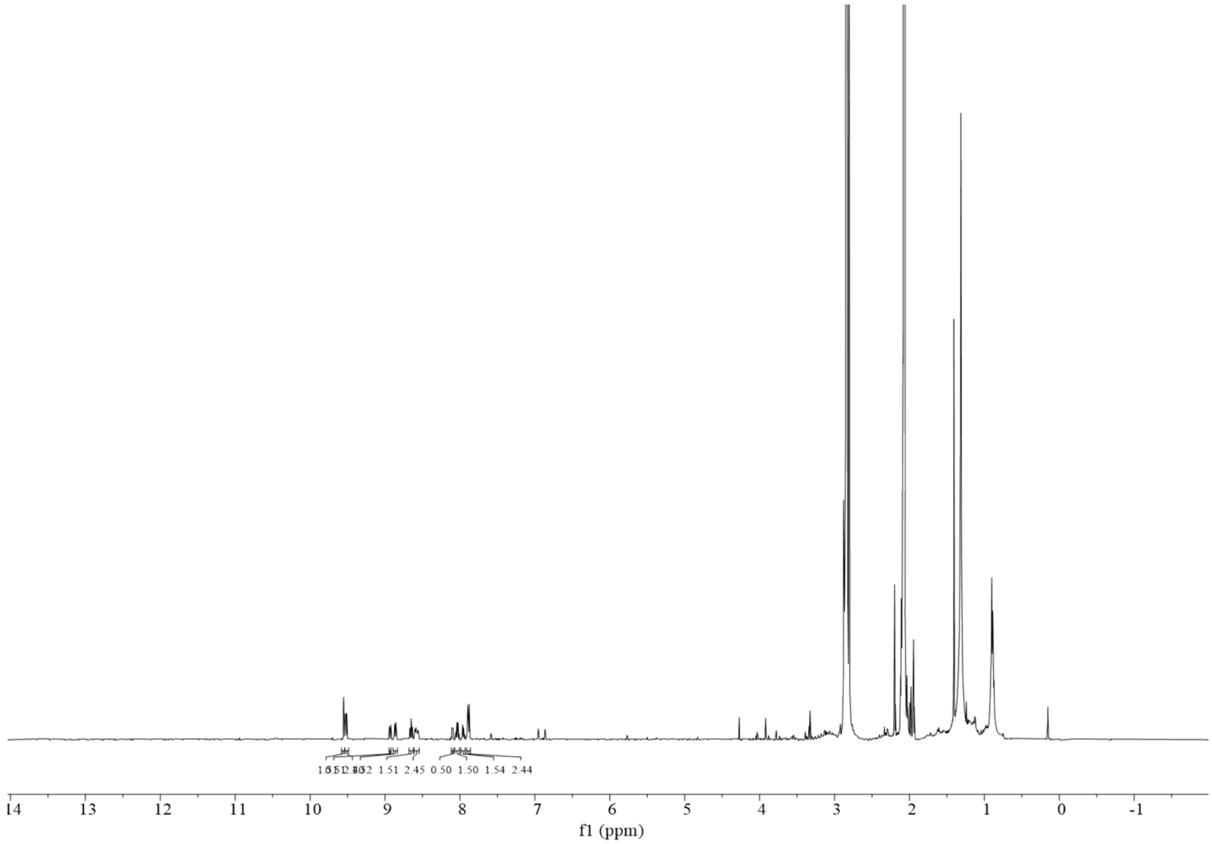

Figure S4. ^{1}H NMR spectrum (500 MHz) of F_5-Cl_nBsubNc band 1.

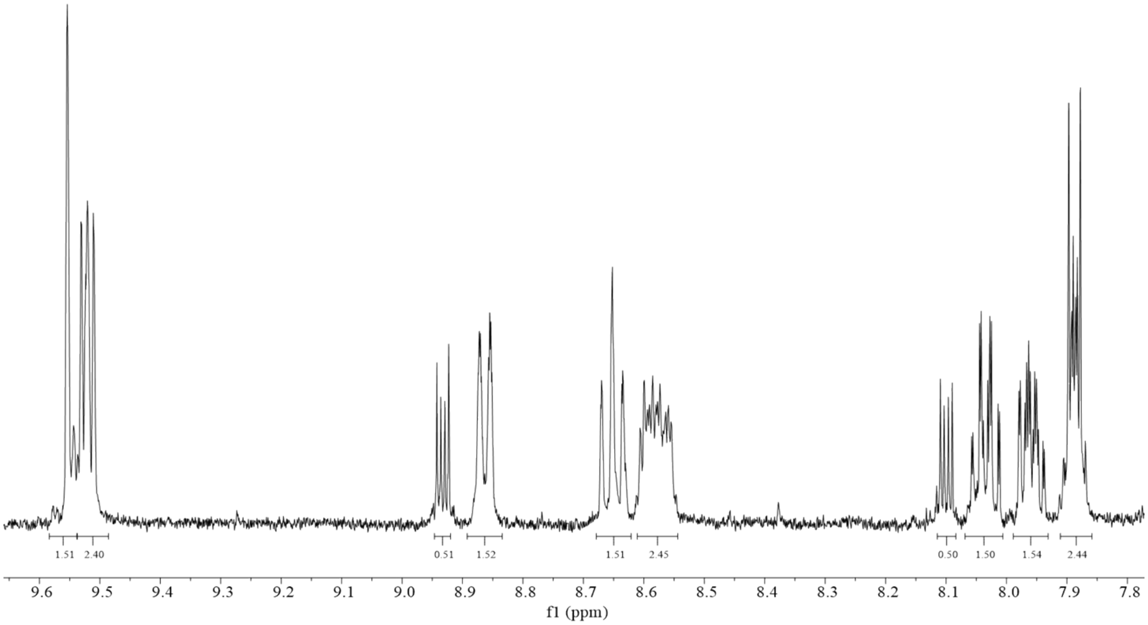

Figure S5. ^{1}H NMR spectrum (500 MHz) zoom of F_5-Cl_nBsubNc band 1.

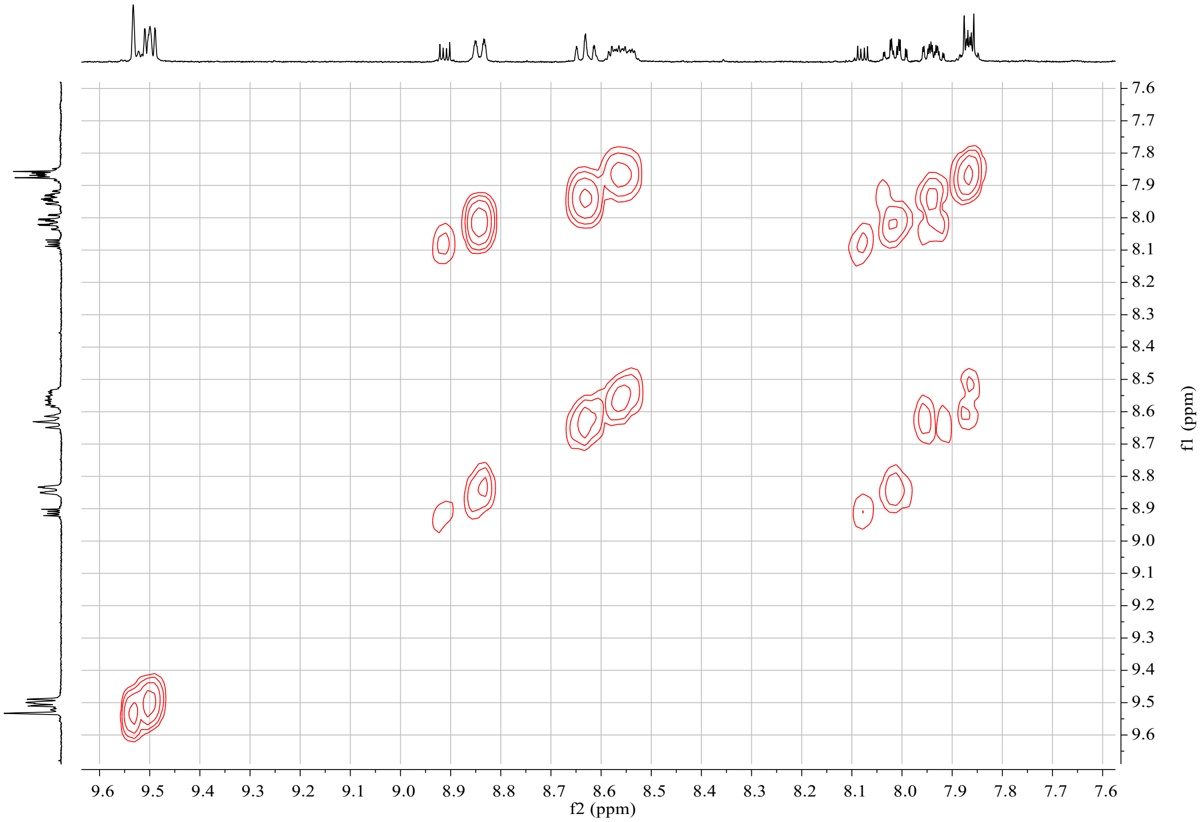

Figure S6. 2D COSY NMR spectrum (500 MHz) of F_5-Cl_nBsubNc band 1.

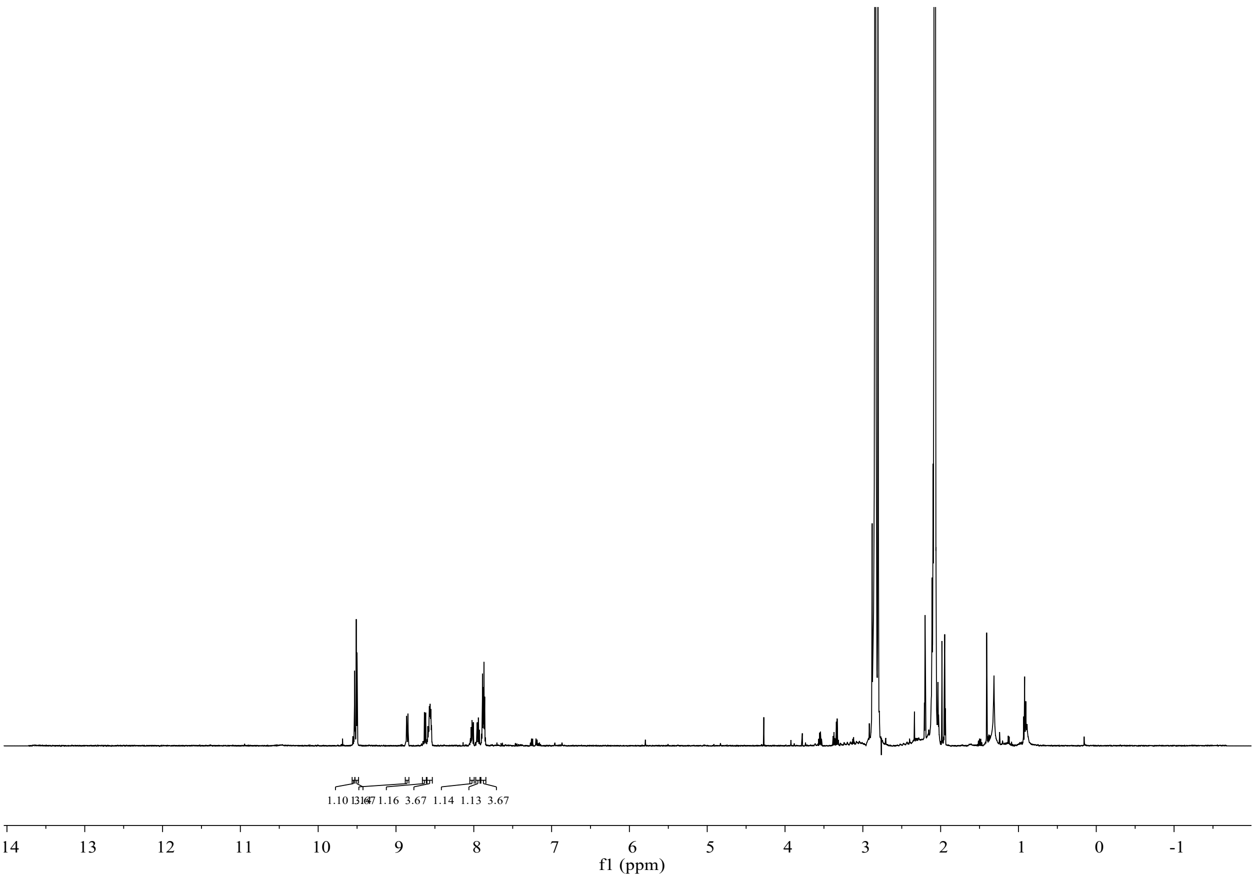

Figure S7. ^{1}H NMR spectrum (500 MHz) of F_5-Cl_nBsubNc band 2.

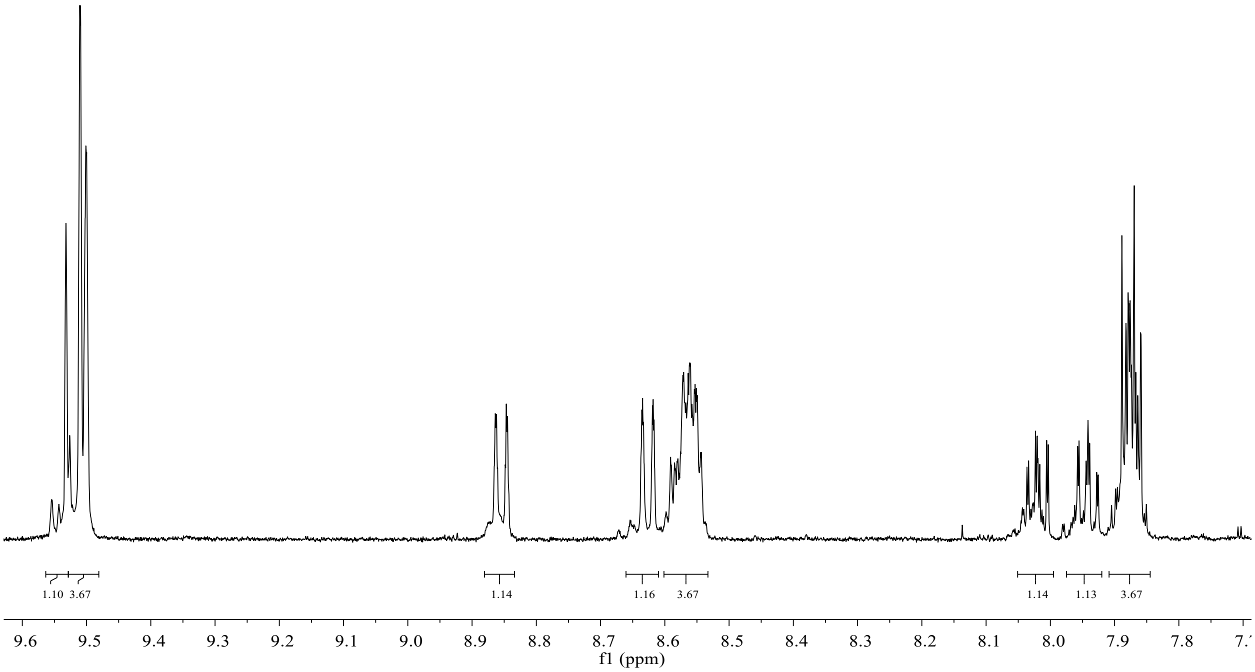

Figure S8. ^{1}H NMR spectrum (500 MHz) zoom of F_5-Cl_nBsubNc band 2.

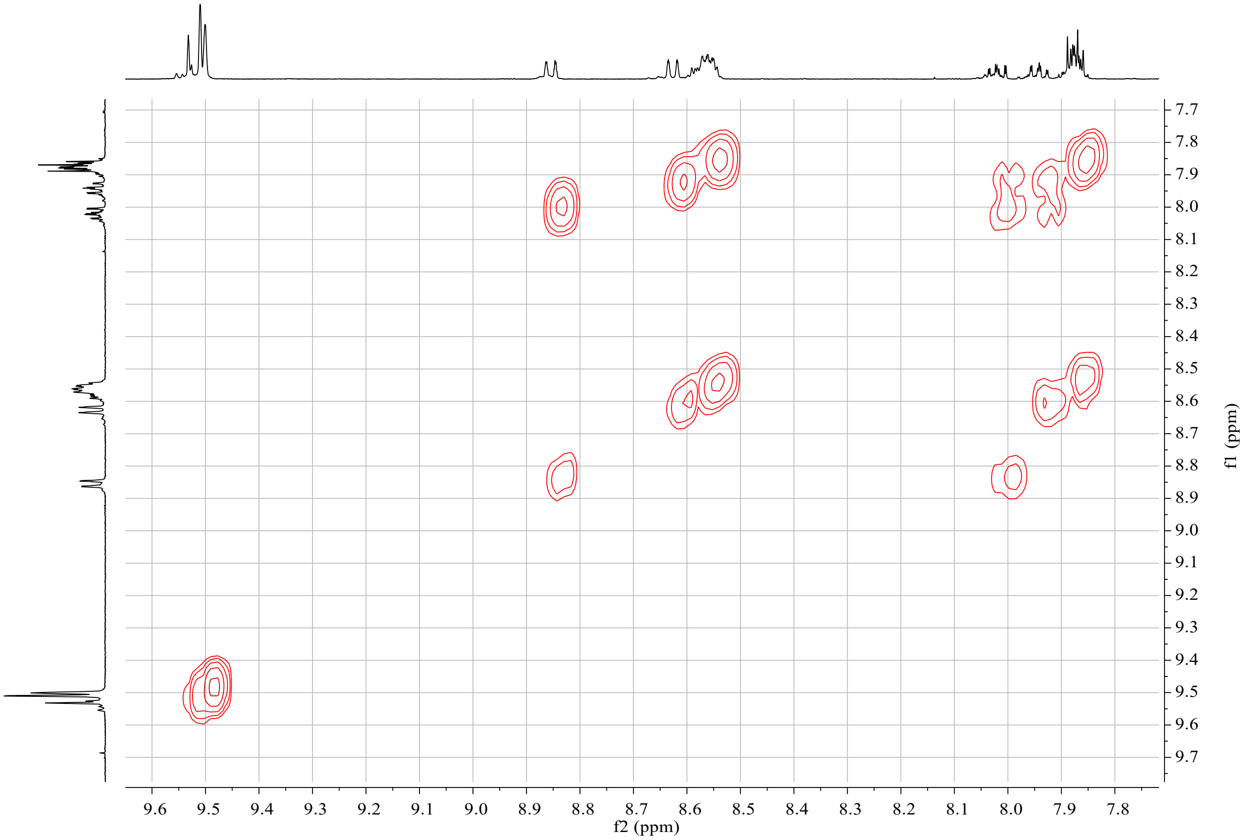

Figure S9. 2D COSY NMR spectrum (500 MHz) of F_5-Cl_nBsubNc band 2.

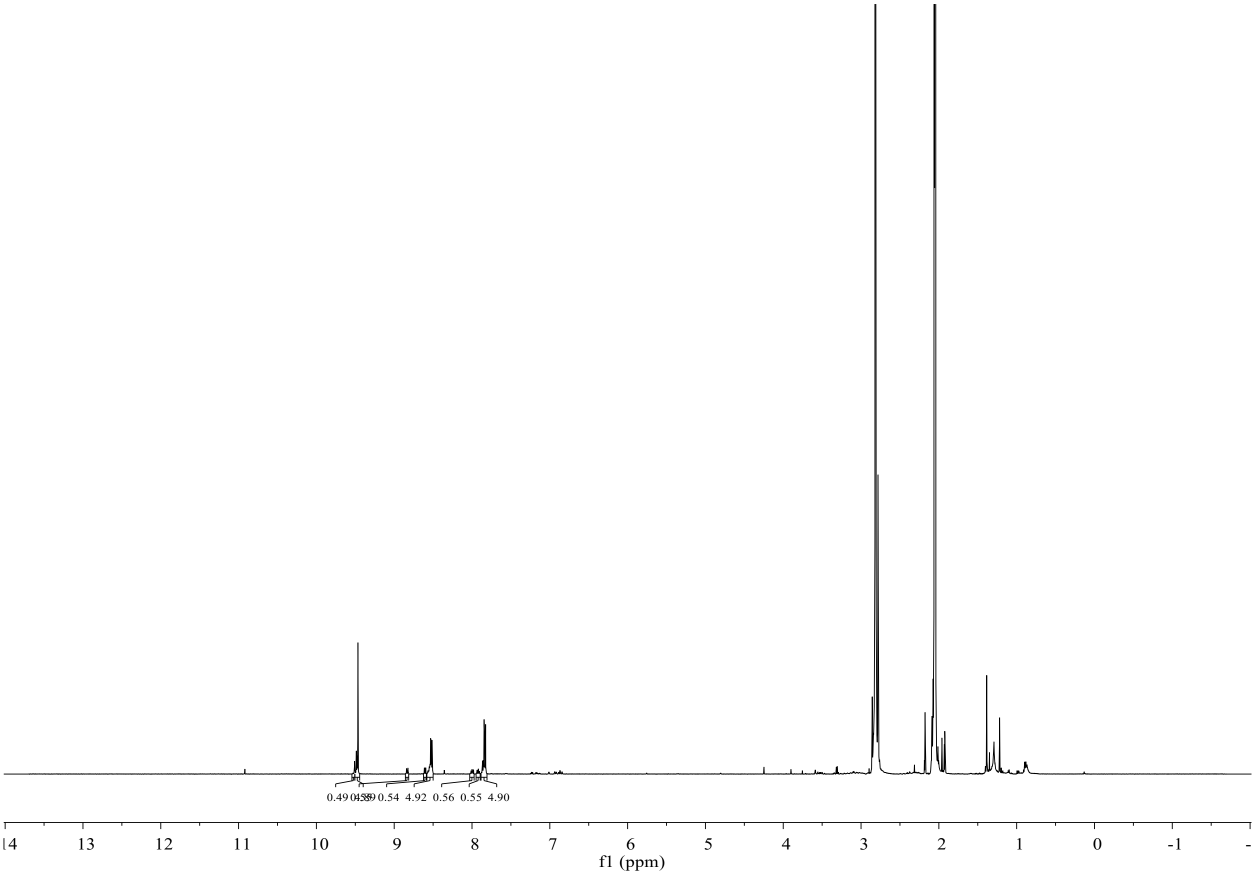

Figure S10. $_1$H NMR spectrum (500 MHz) of F_5-Cl_nBsubNc band 3.

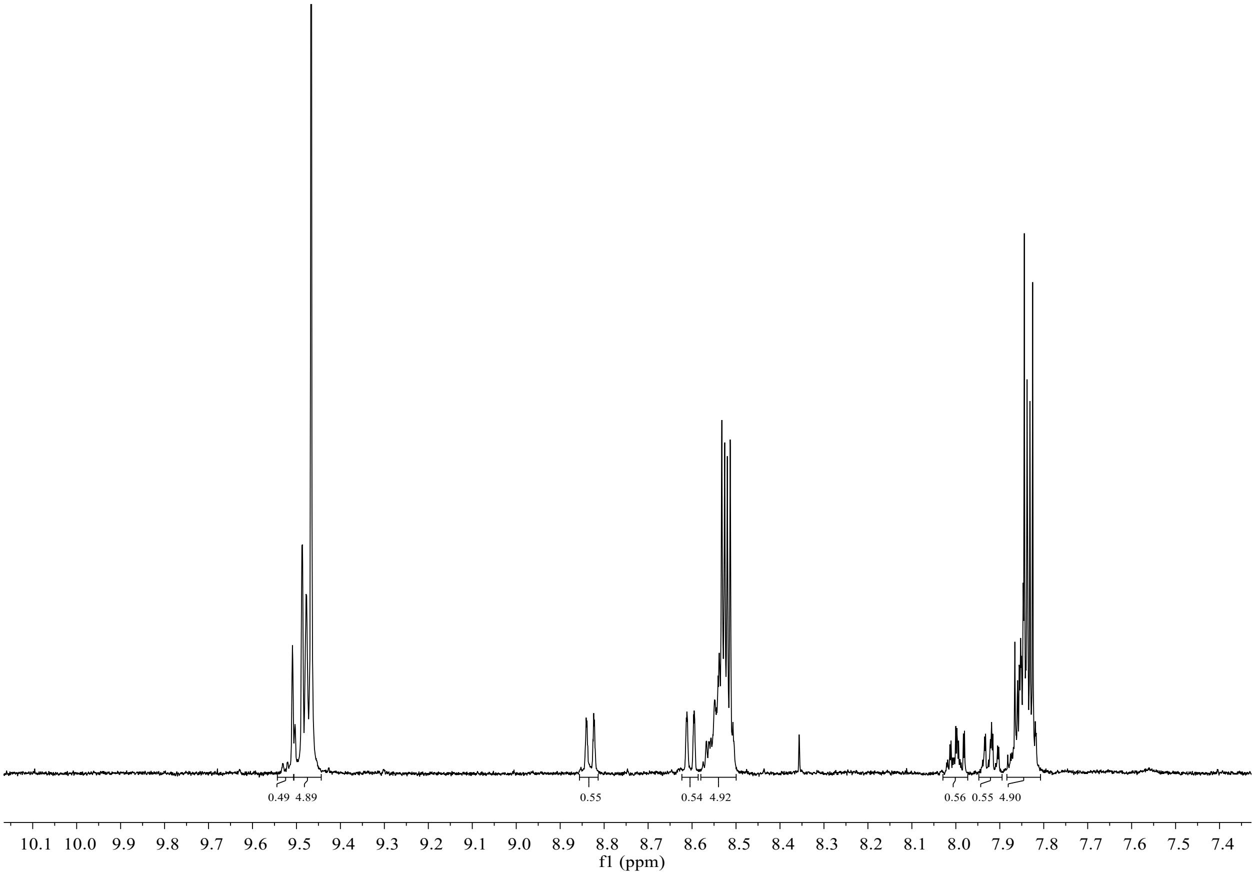

Figure S11. ^{1}H NMR spectrum (500 MHz) zoom of F_5-Cl_nBsubNc band 3.

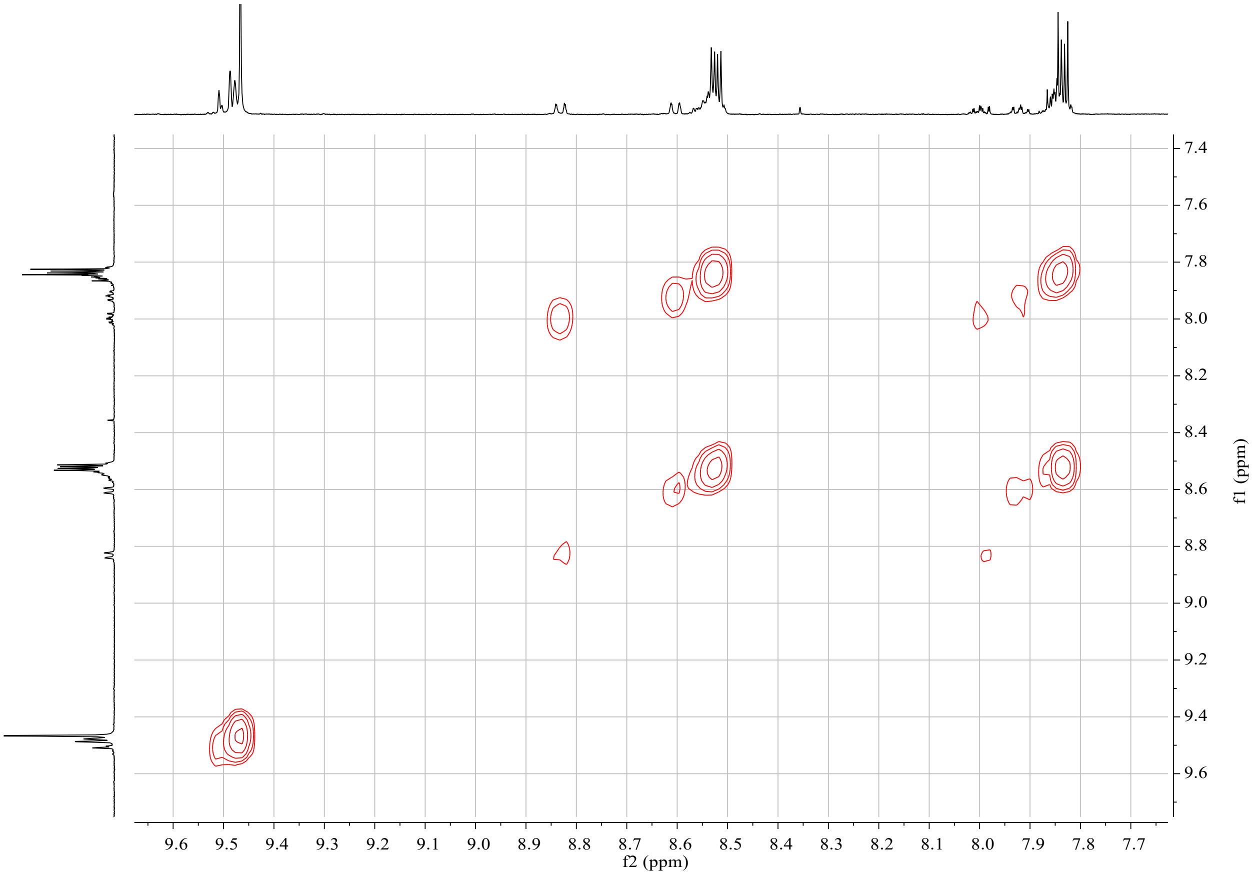

Figure S12. 2D COSY NMR spectrum (500 MHz) of F_5-Cl_nBsubNc band 3.

Mass Spectrometry

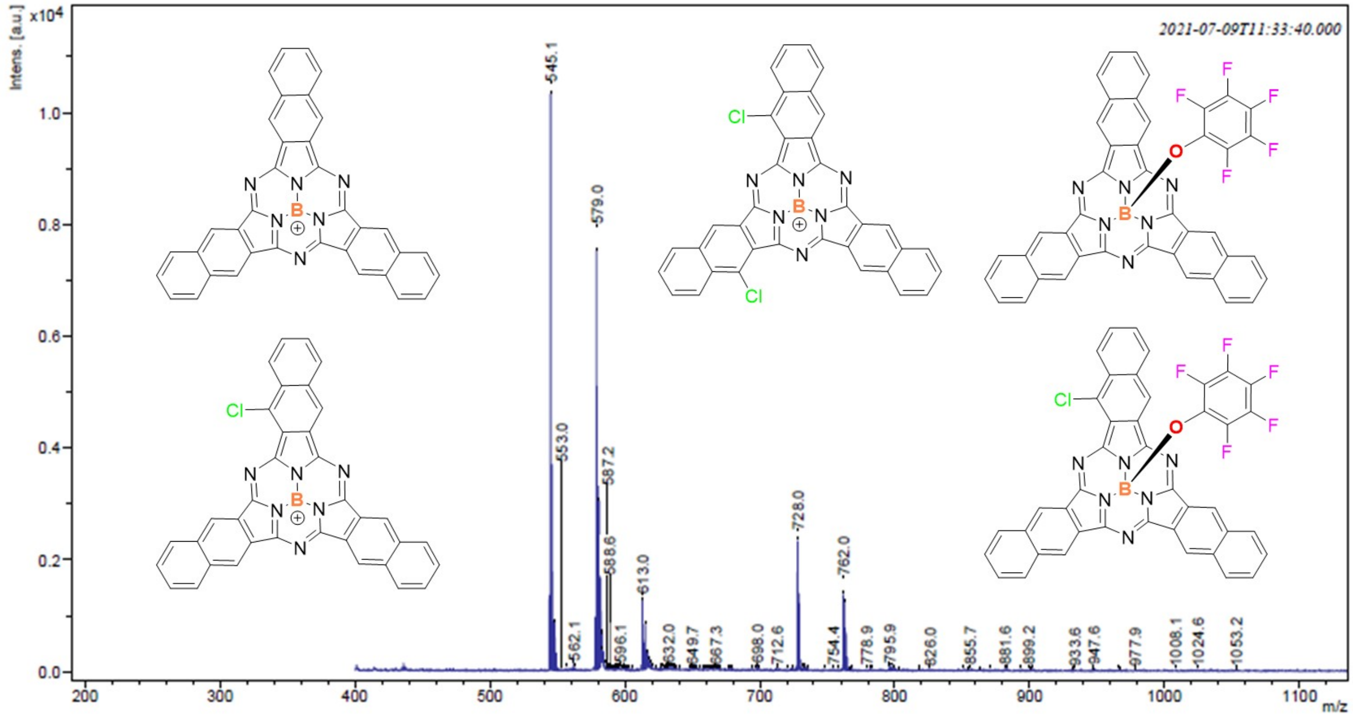

Figure S13. MALDI-MS of F_5-Cl_nBsubNc Crude with DHB as the matrix.

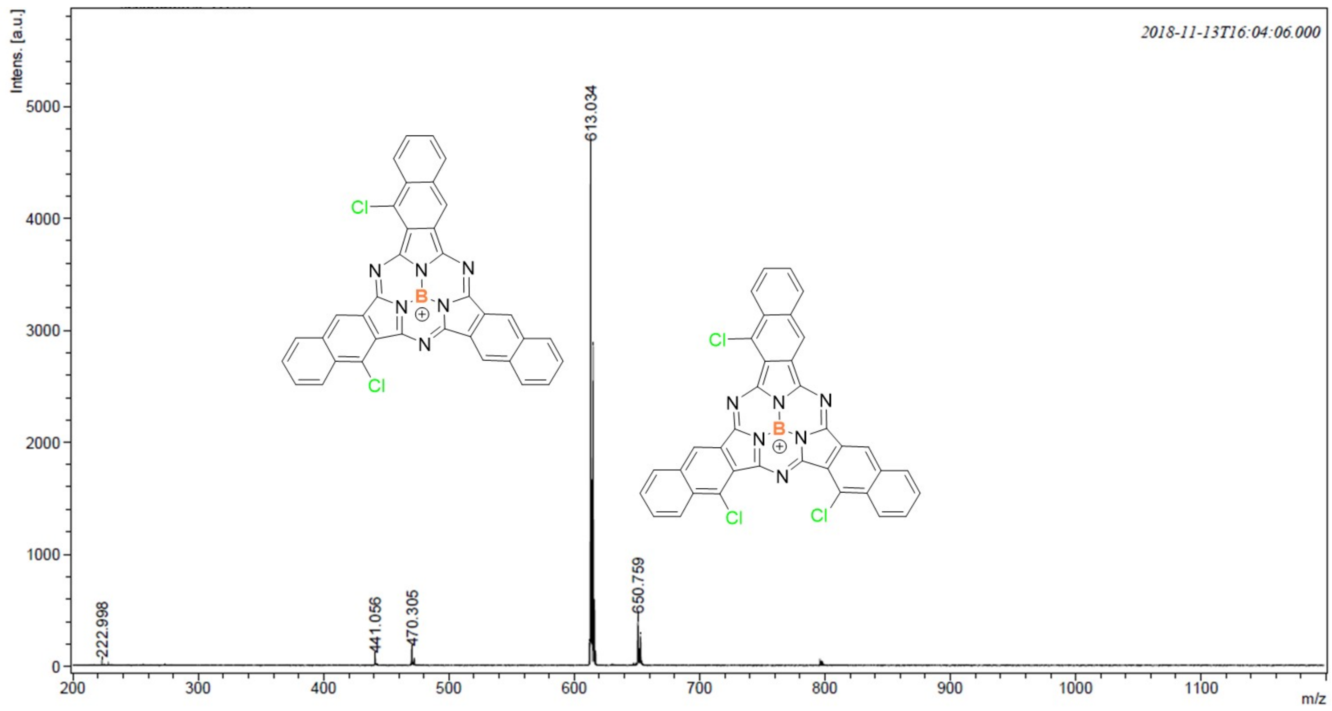

Figure S14. MALDI-MS of F_5-Cl_nBsubNc band 1 with DHB as the matrix.

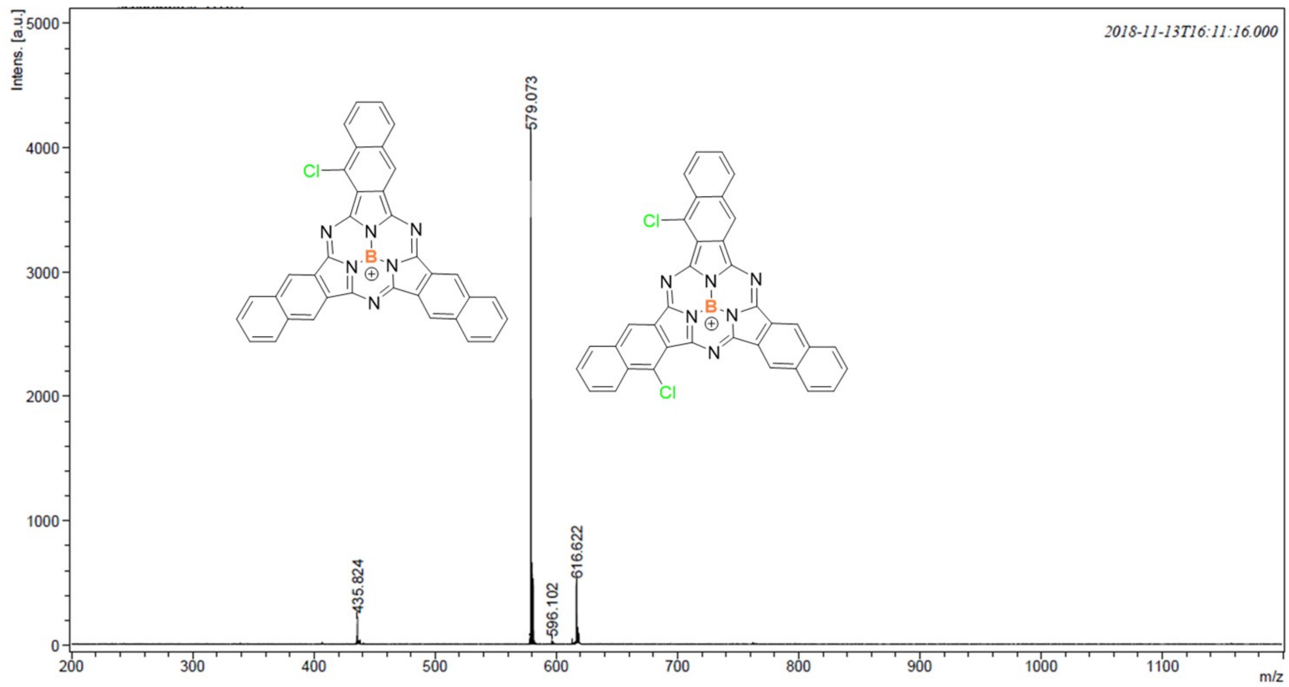

Figure S15. MALDI-MS of F$_5$-Cl$_n$BsubNc band 2 with DHB as the matrix.

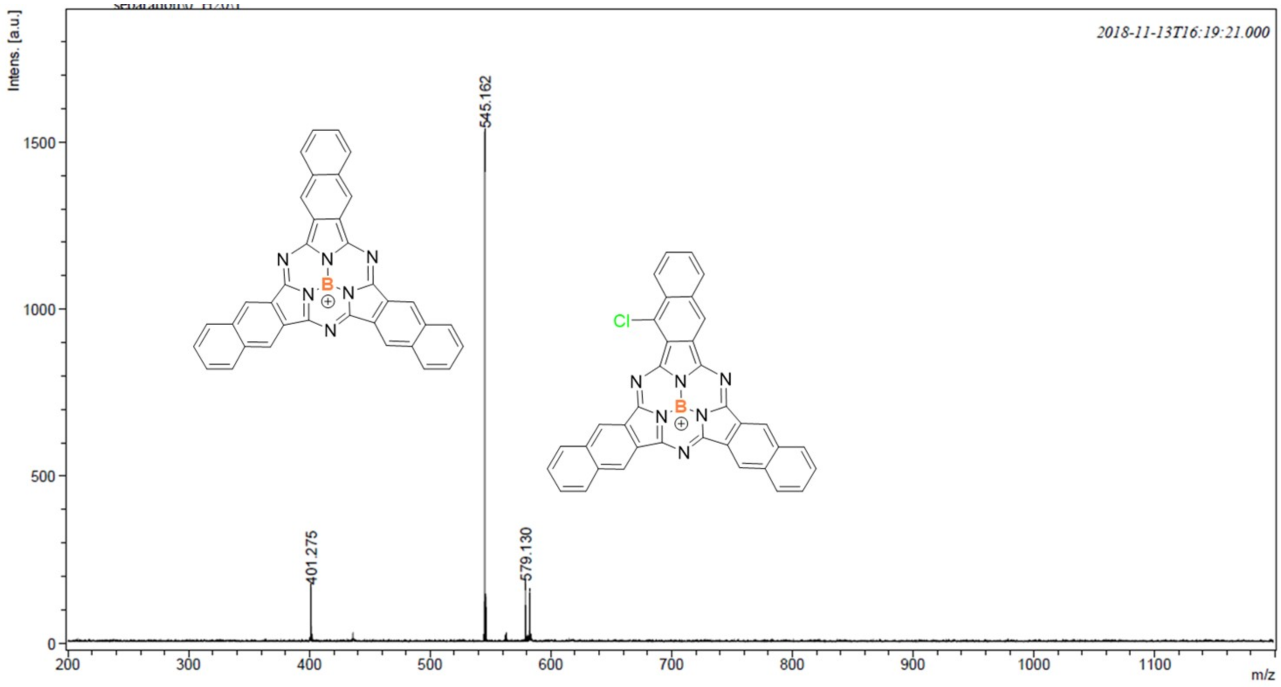

Figure S16. MALDI-MS of F$_5$-Cl$_n$BsubNc band 3 with DHB as the matrix.

Photophysical Experiments

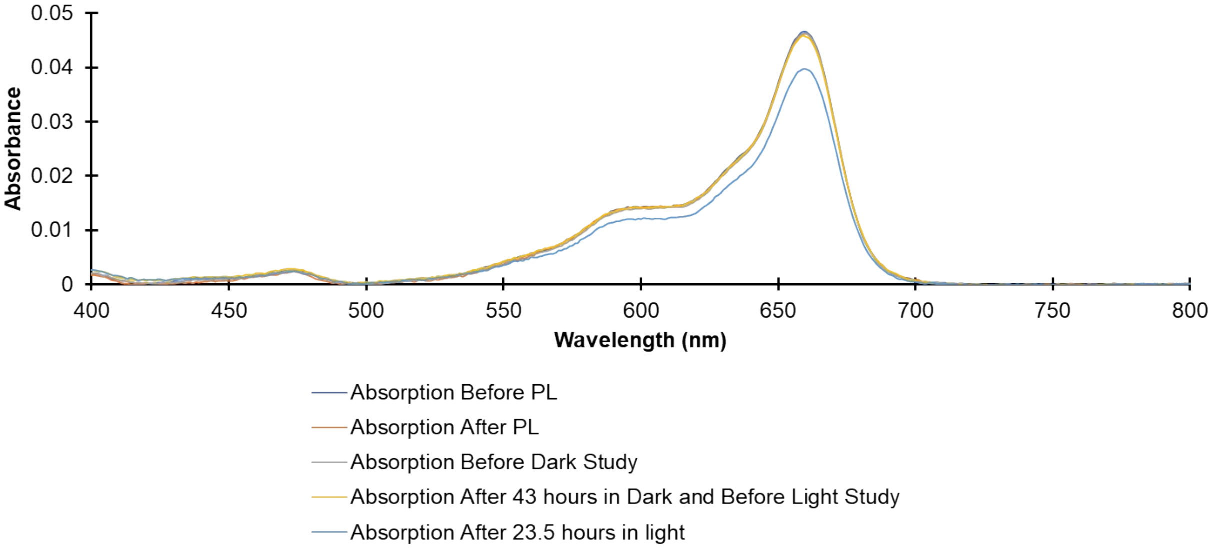

Figure S17. Absorption spectroscopy to measure the solution stability of F_5-Cl_nBsubNc Band 1 in the dark, under ambient light, as well as before and after photoluminescence spectroscopy. Measurements taken in toluene at room temperature.

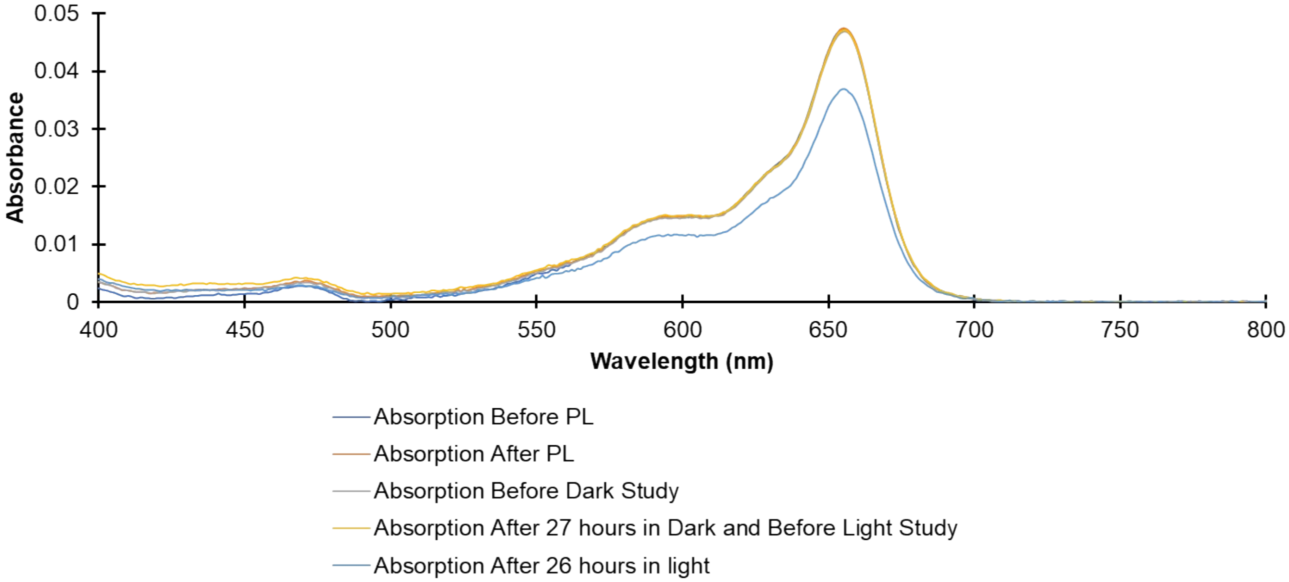

Figure S18. Absorption spectroscopy to measure the solution stability of F_5-Cl_nBsubNc Band 2 in the dark, under ambient light, as well as before and after photoluminescence spectroscopy. Measurements taken in toluene at room temperature.

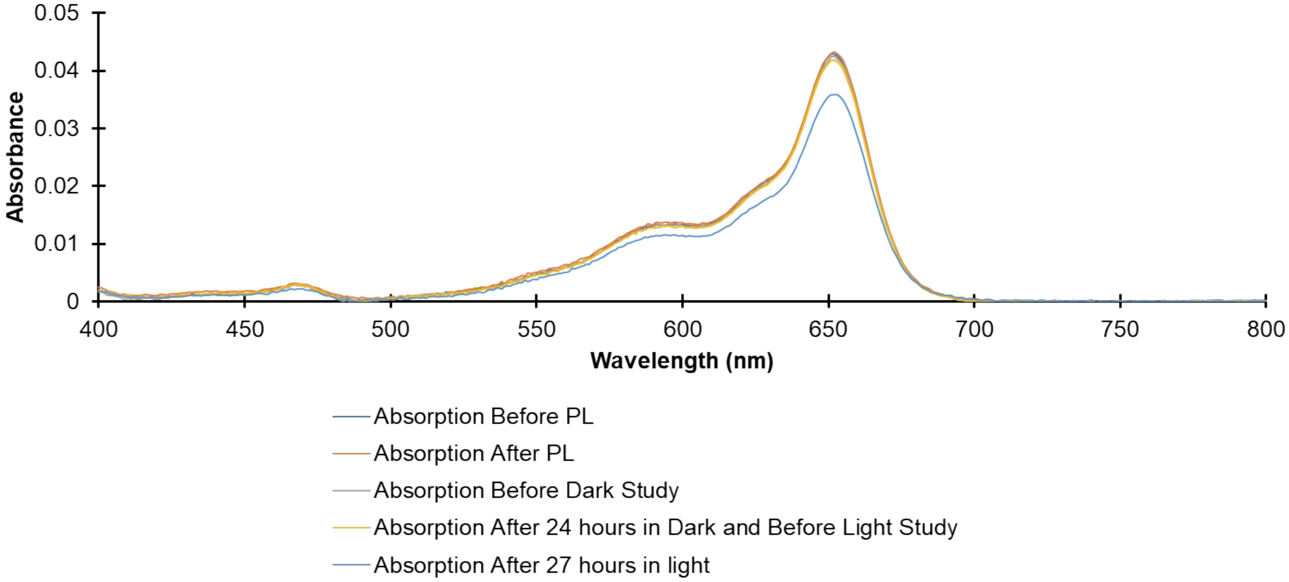

Figure S19. Absorption spectroscopy to measure the solution stability of F_5-Cl_nBsubNc Band 3 in the dark, under ambient light, as well as before and after photoluminescence spectroscopy. Measurements taken in toluene at room temperature.

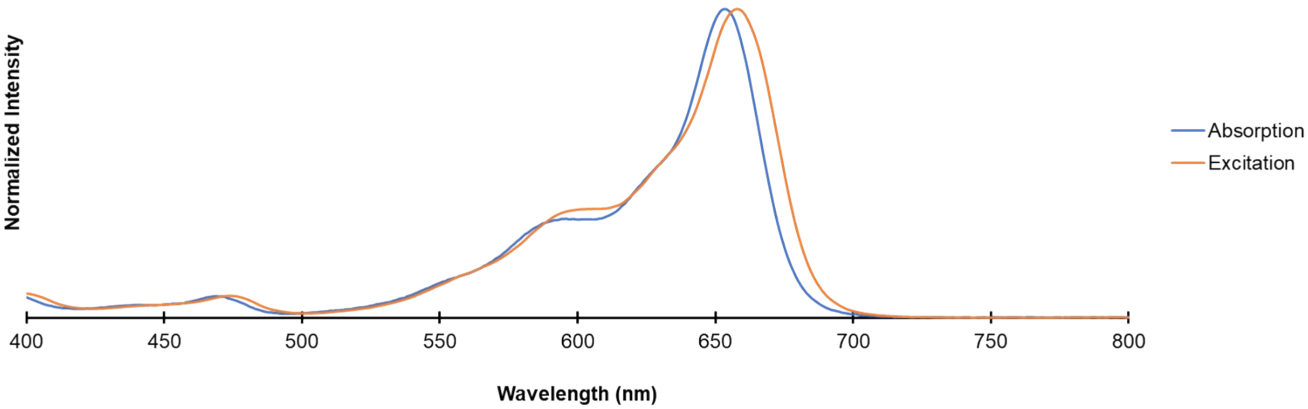

Figure S20. Absorption and excitation spectra overlay of F_5-Cl_nBsubNc in toluene at room temperature.

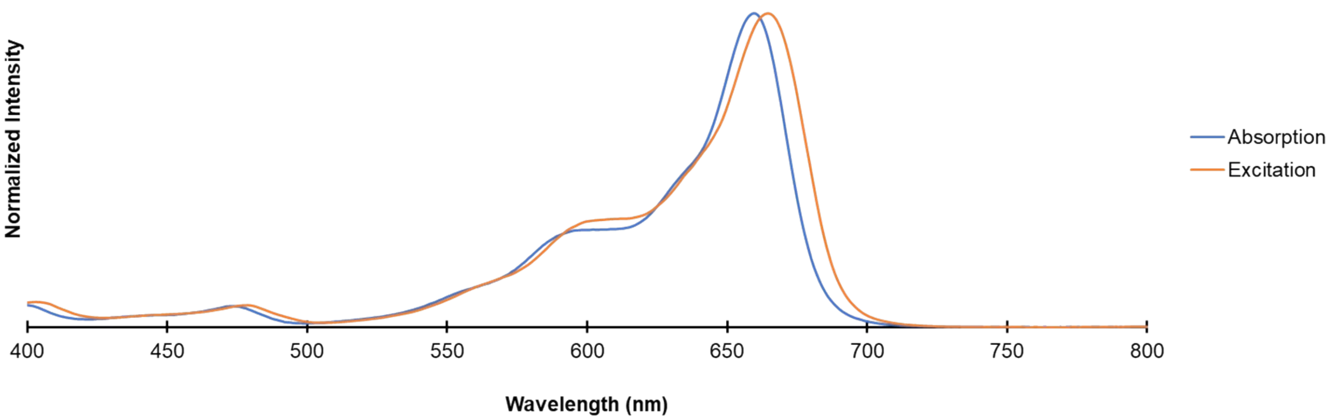

Figure S21. Absorption and excitation spectra overlay of F_5-Cl_nBsubNc band 1 in toluene at room temperature.

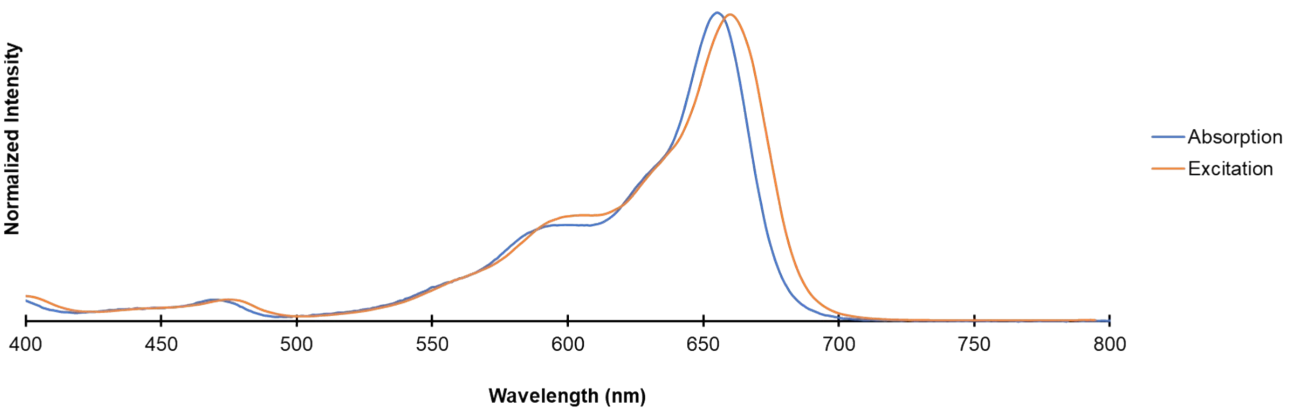

Figure S22. Absorption and excitation spectra overlay of F_5-Cl_nBsubNc band 2 in toluene at room temperature.

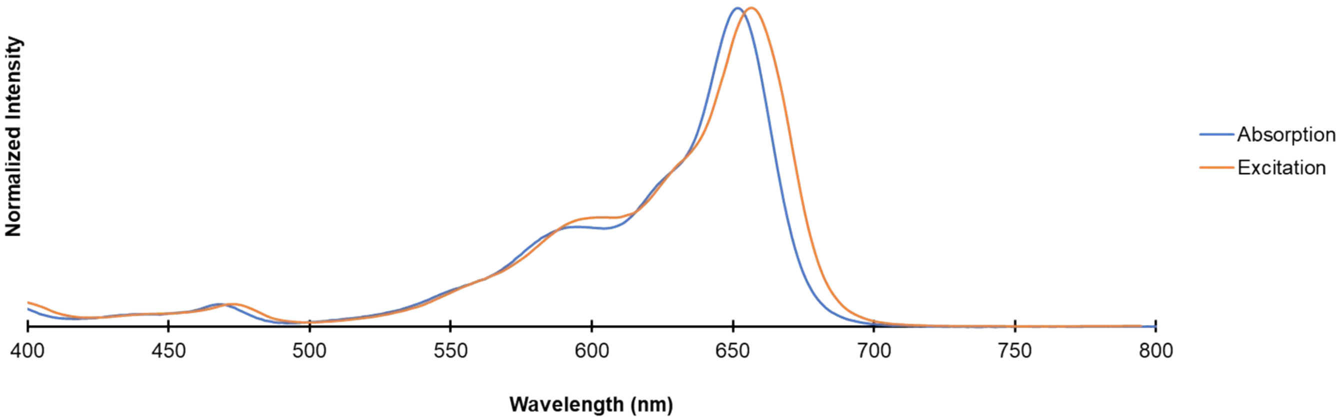

Figure S23. Absorption and excitation spectra overlay of F_5-Cl_nBsubNc band 3 in toluene at room temperature.

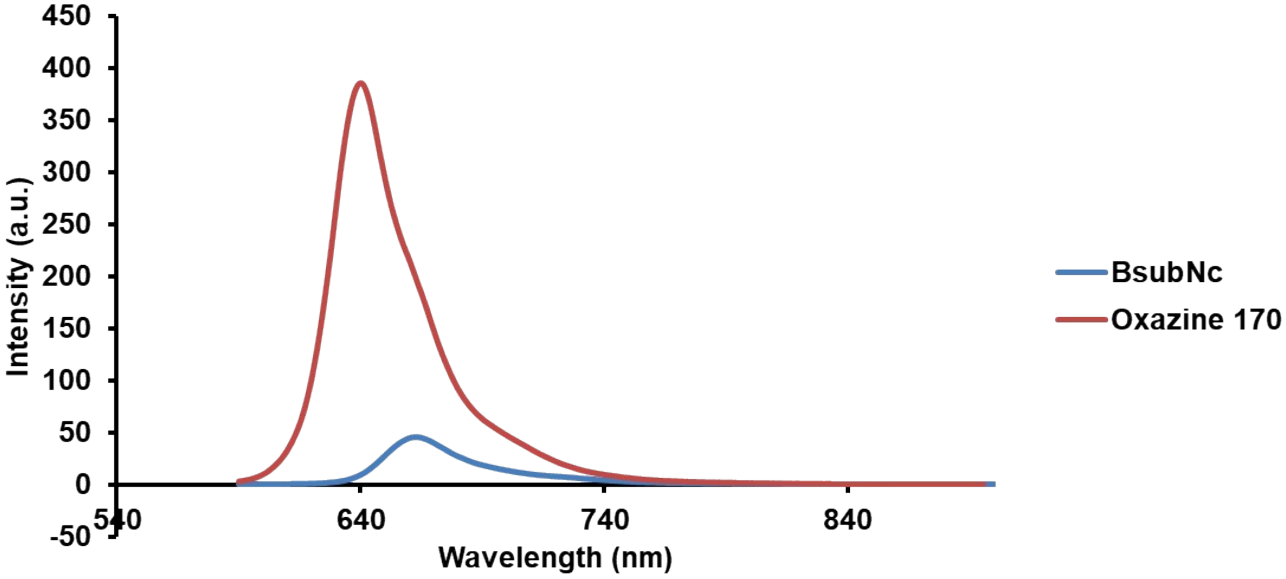

Figure S24. Photoluminescence spectrum of F_5-Cl_nBsubNc crude and the standard oxazine-170 with an excitation wavelength of 580 nm. Reflection peaks removed for clarity.

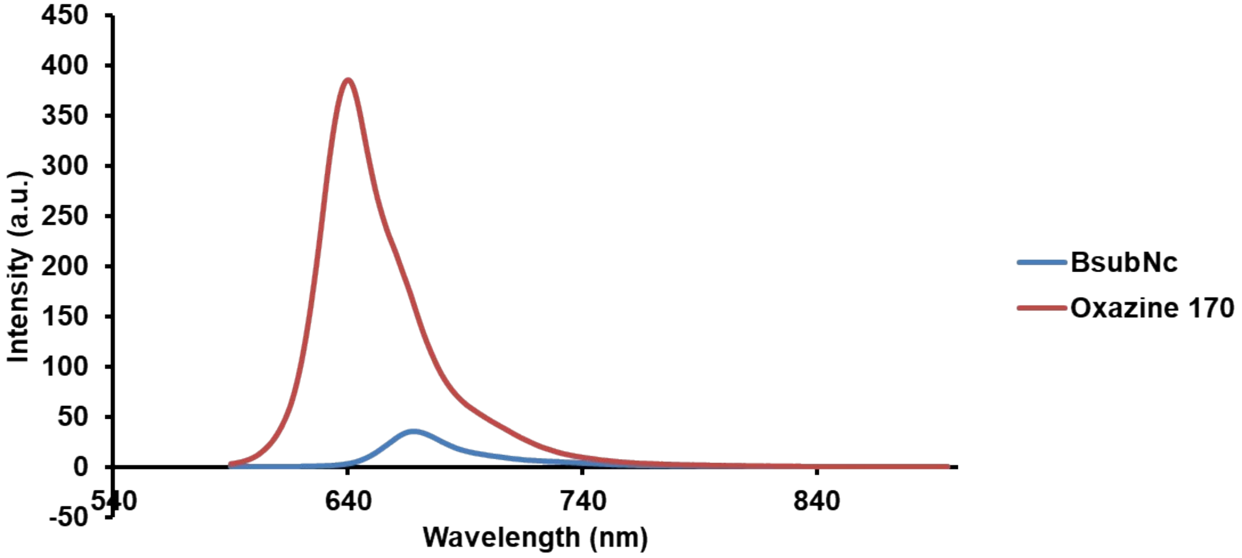

Figure S25. Photoluminescence spectrum of F_5-Cl_nBsubNc band 1 and the standard oxazine-170 with an excitation wavelength of 580 nm. Reflection peaks removed for clarity.

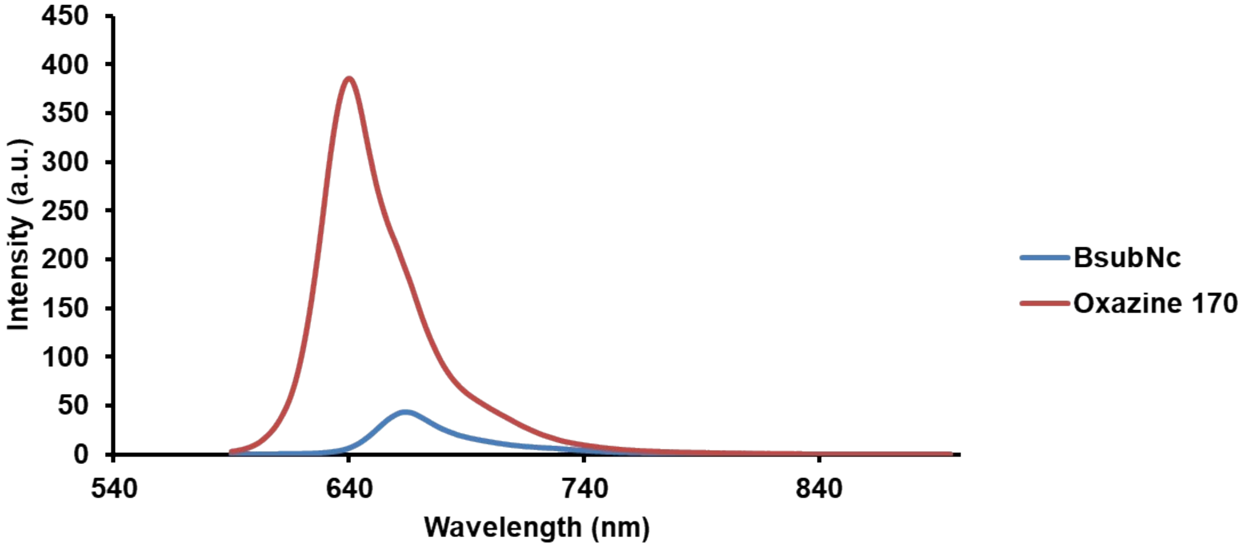

Figure S26. Photoluminescence spectrum of F_5-Cl_nBsubNc band 2 and the standard oxazine-170 with an excitation wavelength of 580 nm. Reflection peaks removed for clarity.

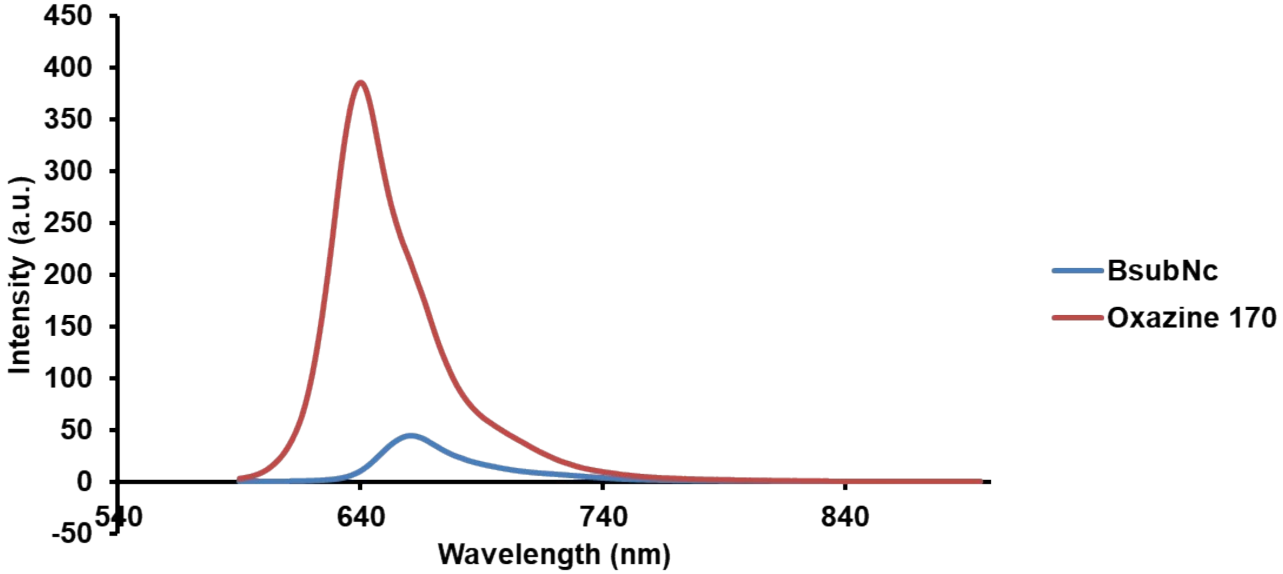

Figure S27. Photoluminescence spectrum of F_5-Cl_nBsubNc band 3 and the standard oxazine-170 with an excitation wavelength of 580 nm. Reflection peaks removed for clarity.

Equations

Fluorescence quantum yield

Fluorescence quantum yields (Φ_{PL}) were calculated using the following formula:

$$\Phi_{PL} = \Phi_R \,(I / I_R)(OD_R / OD)(n^2 / nR^2) \qquad \textbf{(Equation S1.)}$$

where I is the integrated fluorescence intensity, OD is the absorbance, and n is the refractive index of the solvent. The subscript R denotes oxazine 170, the reference fluorophore we used herein, which has previously been reported to have a fluorescence quantum yield of 0.5793[1] in ethanol at room temperature. The analyses of all F_5-Cl_nBsubNc samples were acquired in toluene at room temperature.

Estimation of HOMO energy from the first oxidation halfwave potential

HOMO energies (E_{HOMO}) were estimated from first oxidation halfwave potentials (V_{CV}) using the following equation from D'Andrade *et al.*[2]:

$$E_{HOMO} = -(1.4 \pm 0.1)\, qV_{CV} - (4.6 \pm 0.08)\ \text{eV} \qquad \textbf{(Equation S2.)}$$

where q is the electron charge. The electrochemical analyses of all F_5-Cl_nBsubNc samples utilized a 0.1 M Bu_4NClO_4 as the electrolyte solution in nitrogen degassed anhydrous dichloromethane at room temperature with a 100 mV/s scan rate versus Ag/AgCl and decamethylferrocene as an internal standard.

References

1. K. Rurack and M. Spieles, *Anal. Chem.*, 2011, **83**, 1232-1242.
2. B. W. D'Andrade, S. Datta, S. R. Forrest, P. Djurovich, E. Polikarpov and M. E. Thompson, *Org. Electron.*, 2005, **6**, 11-20.